Master's Thesis of Medicine

Protection against Influenza-Associated Severe Lung Immunopathology through Adeno-Associated Virus Vector Administration

아데노연관바이러스 벡터의 인플루엔자 관련 폐의 중증 면역손상 억제능

August 2023

Graduate School of Medicine
Seoul National University
Translational medicine Major

Eun Ah Choi

Protection against Influenza-Associated Severe Lung Immunopathology through Adeno-Associated Virus Vector Administration

By Eun Ah Choi
(Directed by Prof. Kyeong cheon Jung)

Submitting a master's thesis of
Medicine

April 2023

Graduate School of Medicine
Seoul National University
Translational medicine Major

Eun Ah Choi

Confirming the master's thesis written by
Eun Ah Choi
July 2023

Chair _____(Seal)

Vice Chair _____(Seal)

Examiner _____(Seal)

Abstract

Influenza A viruses (IAV) have long been a threat to humans, occasionally causing high morbidity and mortality. The initial immune response is triggered by infected epithelial cells, alveolar macrophages and dendritic cells, followed by infiltration of innate immune cells that limit viral replication and spread before the emergence of adaptive immunity. However, an exaggerated innate immune response could lead to severe lung injury and even host mortality; in particular, the major pathology observed in the lungs of hosts succumbing to severe influenza is the massive influx of neutrophils and monocytes. In this study, experiments were carried out to find modalities to control lung immunopathology following severe influenza infection. First, when CB17.SCID and NOD.SCID mice were infected with PR8 IAV, NOD.SCID mice, which are defective in monocyte/macrophage development and NK cell function, showed significantly attenuated weight loss and decreased mortality compared to CB17.SCID mice. Flow cytometry analysis revealed that attenuated infiltration of neutrophils and inflammatory monocytes was associated with increased survival of NOD.SCID mice. In addition, transcript levels of many inflammatory cytokine and chemokine genes were significantly lower in the infected lungs of NOD.SCID mice than in the CB17.SCID control. However, *Cxcl14* gene transcripts were more abundant in NOD.SCID lungs. Based on this, an adeno-associated virus

(AAV9) vector was used as a gene delivery system to investigate whether overexpression of the *Cxcl14* gene in the lungs of mice is able to protect the host against lethal influenza infection. Interestingly, inoculation of both AAV9-EGFP control and AAV9-EGFP-mCXCL14 vectors into the airways of mice prior to IAV challenge significantly reduced mouse mortality compared to naive controls that did not receive AAV vectors. Flow cytometric analysis revealed that attenuated neutrophil and trans-macrophage infiltration was associated with better prognosis, while there was no difference in viral gene transcript levels between mice of the three groups. Considering that a previous report suggested that the unique genomic structure of AAV vectors could lead to the generation of double-stranded RNA from the viral genome in the cytoplasm of AAV-transduced cells, resulting in the production of interferon-β in an MDA5-dependent manner, these results invoke the immunoregulatory potential of AAV vectors.

Keyword: Influenza virus, Lung, Immunopathology, Adeno-associated virus,

Student Number: 2020-26026

CONTENTS

LIST OF FIGURES

LIST OF TABLES

LIST OF ABBREVIATIONS

AAV : Adeno- Associated Virus

Cap : capsid

cDNA : complementary DNA

DEG : Differentiated expressed gene

dsRNA : Double-stranded RNA

EGFP : enhanced green fluorescent protein

GC : genomic copies

HA : hemagglutinin

IAV : influenza A viruses

IFN : interferon

ITR : inverted terminal repeat

mCXCL14 : murine – CXCL14

NA : neuraminidase

qPCR: reverse transcription quantitative real-time PCR

Rep : replication

INTRODUCTION

Influenza A viruses (IAVs) are negative-sense, single-stranded RNA enveloped virus with eight segmented genes, subdivided on the basis of haemagglutinin (HA) and neuraminidase (NA) surface glycoproteins, which are the major targets of neutralizing antibodies [1, 2]. These viruses are among the fastest evolving viruses [3]. Point mutations in viral proteins, called 'antigenic drift', allow them to escape immunity acquired through previous infection or vaccination and cause annual outbreaks [2]. IAVs are also capable of swapping segmented genomes between genotypically different viruses, and this genetic reassortment between human and animal viruses is known to have led to the emergence of the 1918 H1N1, 1957 H2N2 and 1968 H3N2 viruses that caused major pandemics in the 20th century [3].

The main causes of severe morbidity and mortality associated with pandemic IAVs are lung injury associated with severe immunopathology and secondary bacterial infection [4]. The main pathology observed in the lungs of hosts with severe influenza is the massive influx of neutrophils and monocytes [5]. The initial immune response to IAV infection is the secretion of interferons by infected epithelial cells, alveolar macrophages and dendritic cells, followed by the recruitment of inflammatory cells such as neutrophils, monocytes/macrophages and natural killer cells, and finally the activation of

adaptive immune cells, which contribute to virus clearance and host recovery [6].

Neutrophils could play both beneficial and deleterious roles during influenza infection [7]. It has been reported that when neutrophils were depleted prior to sublethal infection with IAV, viral growth was not controlled and mortality was increased in mice, and these findings were further supported by subsequent studies [7-9]. Neutrophils could exert a protective effect by producing the antimicrobial peptide mCRAMP and promoting the release of IL-1β in alveolar macrophages [8]. Neutrophils also direct the migration of influenza-specific CD8 T cells to the site of infection and maintain CD8 T cell effector responses [9, 10]. However, another study demonstrated that a transcriptional signature of neutrophil accumulation in influenza-infected lungs could predict lethal from sublethal infections, and that attenuation rather than complete depletion of neutrophils reduced mortality in mice, suggesting that dampening exaggerated neutrophilic inflammation is required to protect hosts from lethal influenza infection [11].

Upon exposure to IAVs, alveolar macrophages promote the recruitment of $CCR2^{+}$ $Ly6C^{high}$ inflammatory monocytes, from which inflammatory monocyte-derived macrophages and inflammatory dendritic cells are differentiated and promote the recruitment of protective NK cells [6, 12]. However, prolonged recruitment of inflammatory monocytes has been reported to contribute to the lethality of severe influenza infection, and

depletion of these cells attenuated lung injury [13, 14]. In contrast to neutrophils and inflammatory monocytes, alveolar macrophages are derived from precursors in the yolk sac and are long-lived in the alveolar space of the lung after birth [15]. These cells exert antiviral activity through recognition of viral RNA and secretion of type I interferon (IFN), and eliminate virus-infected cells by phagocytosis [16]. Alveolar macrophages have been reported to protect alveolar epithelial cells from IAV infection, and depletion of alveolar macrophages caused severe lung injury due to exaggerated neutrophilic infiltration and increased viral load [17-19].

Adeno-associated virus (AAV) is a non-enveloped single-stranded DNA parvovirus with a genome of approximately 4.8 kb, and its non-pathogenic and low immunogenic properties and broad tropism have allowed this virus to be a useful delivery system for long-term expression of therapeutic genes in both animals and humans [20, 21]. In particular, since the successful clinical trials in hemophilia patients more than 10 years ago, many clinical trials with AAV vectors targeting various genetic diseases have been conducted [22]. The AAV genome consists of replication (rep) and capsid (cap) genes, and the ends of the genomic DNA are flanked by two inverted terminal repeats (ITRs) [22, 23]. AAV vectors are constructed by replacing most of the viral genome with expression cassettes consisting of a promoter, a gene of interest and a poly A tail [24]. After AAV vectors are integrated into host cells, the 3'-ITR acts as a primer for the host DNA polymerase and a self-complementary intermediate

containing both plus and minus DNA strands is generated [22, 23]. Interestingly, a previous report suggested that both plus and minus strand RNAs could be copied from the self-complementary intermediate DNA in the cytoplasm of AAV-transduced cells due to the inherent promoter activity of 5'- and 3'-ITRs, resulting in the formation of double-stranded RNA (dsRNA) and thereby triggering a cytoplasmic dsRNA sensor, MDA5 in host cells [25]. In this situation, the sensing of dsRNA led to the production of IFN-β, which subsequently suppressed transgene expression. However, it has not been investigated whether in vivo gene transduction with AAV vectors itself could also influence the other immune response, for example in response to IAV infection.

Here, CB17.SCID and NOD.SCID mice were first used to explore the strategy for controlling lung immunopathology after severe influenza infection, and it was found that attenuated infiltration of neutrophils and inflammatory monocytes was associated with reduced morbidity and mortality in NOD.SCID mice compared to CB17.SCID. In addition, *Cxcl14* chemokine gene expression levels were higher in NOD.SCID lungs than in the CB17.SCID control after IAV infection. AAV9 was then used to test whether overexpression of CXCL14 in BALB/c lungs could protect the host against lethal influenza infection. Interestingly, mortality after IAV challenge was significantly reduced in mice receiving AAV9 vector, regardless of the type of gene delivered (*Cxcl14* vs. control genes), compared to mice not receiving

AAV9 vector. Further analysis revealed that the increased survival was associated with reduced neutrophil and trans-macrophage infiltration in the infected lungs. These results demonstrated the immunoregulatory potential of AAV vectors.

MATERIALS AND METHODS

1. Subjects

BALB/c, NOD.SCID and CB17.SCID mice were purchased from Jackson Laboratories (Bar Harbor, ME, USA). All mice were obtained from the laboratory animal facility of the Biomedical Center for Animal Resource Development at Seoul National University. Mice were housed in sterilized cages and provided with sterilized food and water. The wild-type and immunodeficient mice were used at the age of 6 weeks and the mean body weight was 18 g. This study was approved by the Institutional Animal Care and Use Committee (IACUC) of the Seoul National University Institute of Laboratory Animal Resource (IACUC number: 220221-3-2). All experiments were performed in accordance with international and institutional guidelines.

2. Experimental group and monitoring

To compare the severity of IAV infection in SCID, CB17.SCID and NOD.SCID mice were infected intranasally with IAV. For the AAV9 vector experiment, BALB/c mice were divided into two or three groups as follows: The naive group was untreated, group 2 was inoculated with AAV9-EGFP only and group 3 was inoculated with AAV9-EGFP-mCXCL14 containing the murine *Cxcl14* gene. These mice were then

infected with IAV 2 or 4 weeks later. All mice were weighed daily after IAV infection. Some mice were sacrificed 1-5 days after IAV infection for analysis of inflammatory cell infiltration and gene expression in the infected lungs.

3. Virus preparation, AAV production, infection, and tissues harvest

Influenza A virus (IAV) strain A/PR/8/34 (PR8, H1N1) was used in this study. Viral stocks were obtained by transfection of MDCK cells as provided by the laboratory of Pr. YK Choi's laboratory (Chungbuk National University, Chungbuk, Korea). The virus was harvested 24 h after transfection and frozen at -80℃ until use. During infection, mice were anaesthetized with isoflurane and O_2. Mice were infected intranasally with 50 µl of PBS containing PR8 virus at a dose of 3.5 x 10^5 PFU/ml. This approach ensures that the virus is deposited in the lower respiratory tract. AAV9-EGFP and AAV9-EGFP-mCXCL14 vectors were purchased from Vector Builder (Chicago, Illinois, USA) in $2x10^{13}$ stock and administered oropharyngeally to mice under anesthesia. A pipette was used to give a bolus inoculation of 50 µl of 10^{12} GC (genome copies) per milliliter of AAV-GFP. Infection was performed in a biosafety level 2 laboratory according to the animal facility guidelines of the Biomedical Research Institute of Seoul

National University Hospital (Seoul, Korea). Lung tissues were harvested with PBS and cut with a razor, and dissociation medium was prepared by adding 50 μl ul of collagenase type IV (0.1 g/ml, Worthington Biochemical Corporation, NJ, USA) and 50 μl ul of DNase I solution (1 mg/ml, Sigma, St. Louis, Missouri, USA) to 50 ml of RPMI 1640 medium and incubated at 37°C for 2 hours on a shaking platform.

4. Preprocessing and analysis of Bulk RNA-Seq data and gene enrichment

Infected lungs from euthanized mice were homogenized with DMEM, and lung tissue was used for RNA isolation using an RNA isolation kit (BIO-52072, Meridian Bioscience, Memphis, TN, USA). Next-generation sequencing (NGS) was performed using Illumina NovaSeq at Macrogen (Seoul, South Korea). Clean reads were mapped to the genome. Transcripts were assembled and merged in StringTie v2.1.3b according to the annotation corresponding to the genome we used. The genes with *P* value less than 0.05 and fold change greater than 2 were selected for gene set enrichment analysis in Enrichr (https://maayanlab.cloud/ Enrichr/).

5. Flow cytometry analysis

Mononuclear cells were isolated from the lungs of infected or uninfected mice. The samples were stained with the following monoclonal antibodies: Ly6G (1A8), CD11b (M1/70), CD11c (N418), CD49b (DX5), F4/80 (BM8), CD45.2 (104), CD64 (X54-5/7.1), Siglec F (E50-2440), Ly6C (HK1.4). These antibodies were obtained from BD Bioscience (San Jose, CA, USA), eBioscience (San Diego, CA, USA) and BioLegend (San Diego, CA, USA). For surface staining, prepared cells were resuspended in staining buffer (PBS, 0.5% BSA and 0.5mM EDTA) and single cell suspensions were labelled with antibodies for 30 min at 4℃. Phenotypes were determined by flow cytometry on an LSRFortessa X-20 (BD Bioscience, CA, USA). All data were analyzed using FlowJo software v10 (TreeStar, San Carlos, USA.

6. Quantitative Real-Time PCR

Lung tissue was processed for total RNA extraction using Total RNA Isolation Kit (BIO-52072, Meridian Bioscience) according to the manufacturer's instructions. cDNA was synthesized from the extracted RNA using AccuPower Cycle Script RT PreMix (Bioneer). The expression levels of the IAV gene (NS, M), CCL2, CCL20, CXCL1, CXCL2, CXCL5, CXCL11, CXCL14 and glyceraldehyde-3-phosphate dehydrogenase (GAPDH) genes in control and infected mice were assessed by qPCR analysis.

The primer sequences used for qPCR are listed in Table 1. The real-time PCR reaction contains 1 µl of cDNA (0.5 µg/µl), 1 µl of each primer and 5 µl of PowerUp SYBR Green Master Mix (A25742, Applied Biosystems, Framingham, MA, USA). A CFX Connect real-time PCR (Applied Biosystems) was used for qPCR. The PCR program consisted of incubation at 95°C for 10 m, followed by 40 cycles of 15 s at 95°C and 60 s at 60°C, and 95°C for 15 s, 60°C for 60 s, 95°C for 15 s. Gene expression levels were quantified using SYBR-Green and the relative expression of RNA was normalized to its internal control, GAPDH.

Statistics

Statistical analysis was performed using GraphPad Prism, version 8.0 (GraphPad Software Inc., San Diego, CA, USA). Data are presented as mean of experimental measurements and standard deviation (SD). All analytical data were tested for statistical significance using t-test. Differences between groups were considered statistically significant when *p* values were less than 0.05.

Table 1. Sequences of primers (mouse) used for qPCR

Primer	Forward (5'-3')	Reverse (5'-3')
M	CGCTCAGACATGAGAACAGAATGG	TAACTAGCCTGACTAGCAACCTC
NS	CAGGACATACTGATGAGGATG	GTTTCAGAGACTCGAACTGTG
CCL2	CCGGCTGGAGCATCCACGTGT	TGGGGTCAGCACAGACCTCTCTCT
CCL20	CGACTGTTGCCTCTCGTACA	GAGGAGGTTCACAGCCCTTT
CXCL1	CACAGGGGCGC CTATCGCCAA	CAAGGCAAGCCTCGCGACCAT
CXCL2	ACCCCACTGCGCCCAGACAGAA	AGCAGCCCAGGC TCCTCCTTTCC
CXCL5	GCATTTCTGTTGCTGTTCACGCTG	CCTCCTTCTGGTTTTTCAGTTTAGC
CXCL11	GGCTTCCT TATGTTCAAACAGGG	GCCGTTACTCGGGTAAATTACA
CXCL14	CCAAGATTCGCTATAGCGAC	CCTGCGCTTCTCGTTCCAGG
GAPDH	TCACCACCATGGAGAAGGC	GCTAAGCAGTTGGTGGTGCA

RESULTS

Reduced lung inflammation in NOD.SCID compared to CB17.SCID

To assess the role of innate and adaptive immunity in influenza-associated lung injury, BALB/c, CB17.SCID and NOD.SCID mice were used in this study. SCID mice ($Prkdc^{scid}$) lack both T and B cells due to a mutation in an enzyme critical for T cell receptor (TCR) and immunoglobulin gene rearrangement and double-strand break repair [26]. In addition, NOD.SCID mice have some defects in innate immunity, such as altered macrophage development and impaired NK cell function [27, 28]. These three groups of mice were intranasally infected with a sublethal dose of PR8 HIN1 IAV and then monitored for changes in body weight and mortality. Body weight decreased progressively in all these mice after influenza challenge, and no difference in weight loss was found between BABL/c and CB17.SCID mice during the first 6 days (Fig. 1A). During the subsequent period, all BALB/c mice recovered body weight and eventually survived, whereas all CB17.SCID mice failed to recover, resulting in 100% mortality as expected (Fig. 1B). However, NOD.SCID mice showed significantly slower weight loss and longer survival than CB17.SCID mice (Fig. 1 A and B). This raised two possibilities: reduced viral replication or attenuated lung inflammation in NOD.SCID mice compared to the other mice. To assess the first possibility, virus titer was measured by plaque assay using homogenized lung tissue at

day 5 post-infection. As shown in Figure 1C, no difference was found in the viral titer of these three groups of mice.

Next, the inflammatory response in infected lungs at day 1 and 5 post-infection was evaluated by flow cytometric analysis (Fig. 2A), and an attenuated infiltration of inflammatory cells was observed in NOD.SCID lungs compared to CB17.SCID lungs (Fig. 2B). However, granulocytes and inflammatory monocytes showed different kinetics. The number of neutrophils and eosinophils was significantly lower in NOD.SCID mice than in CB17.SCID controls on day 1 post-infection, and the difference between the two groups was progressively reduced during the course of lung inflammation. On the contrary, similar numbers of $CCR2^{+}$ inflammatory monocytes initially infiltrated the lungs of both groups, but the number of infiltrating cells decreased more rapidly in the NOD.SCID lung compared to the CB17.SCID control. Inflammatory monocytes and neutrophils are known to cause lethal lung injury in influenza and SARS-CoV infection [13, 29]. It has also been reported that CCR2 blockade reduces lung pathology associated with influenza infection, and partial suppression of the neutrophil response could also increase survival of mice exposed to lethal IAVs [11, 19]. Taken together, attenuated inflammatory monocyte and neutrophil infiltration in NOD.SCID may contribute to prolonged survival in mice.

Unlike granulocytes and inflammatory monocytes, alveolar

macrophages, which are long-lived in the lung alveolar space after birth, are usually depleted after influenza infection and replaced by bone marrow-derived trans-macrophages [14, 15]. Consistent with this, the number of alveolar macrophages progressively decreased in the infected lungs of both groups, although NOD.SCID mice have a lower number of cells in the early days of infection than CB17.SCID (Fig. 2C). Alveolar macrophages normally play a protective role in influenza infection and have been reported to protect alveolar epithelial cells from IAVs infection [18, 30]. Thus, alveolar macrophages may not be the major player causing early lethality in CB17.SCID mice.

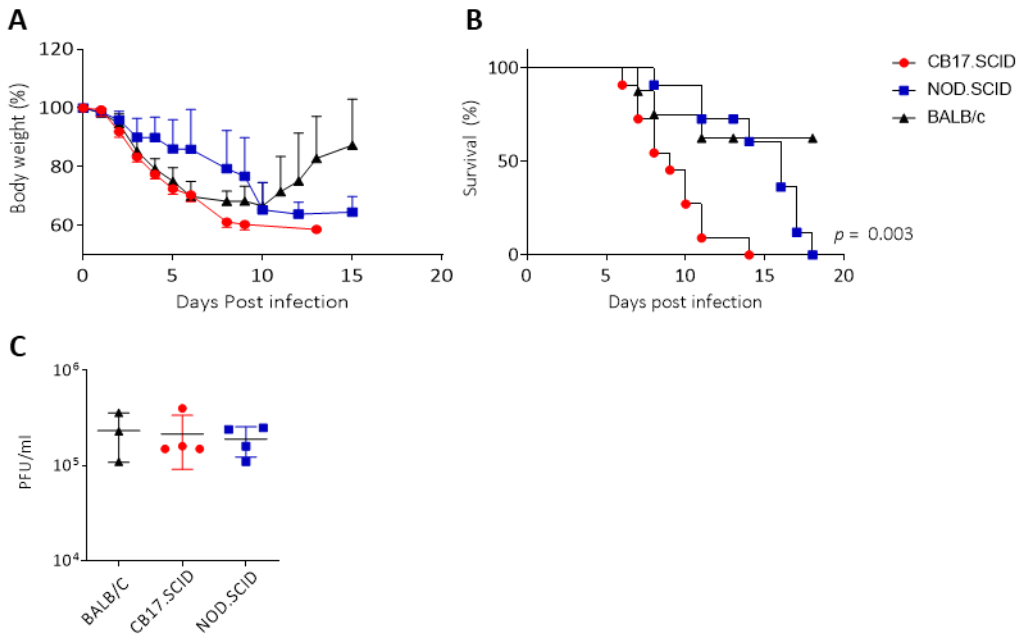

Figure 1. Better prognosis in NOD.SCID mice than CB17.SCID mice after IAV infection. **(A-B)** BALB/c, CB17.SCID and NOD.SCID mice were infected with PR8 virus and body weight (A) and mortality (B) were monitored. Cumulative results of three independent experiments (n=15 per group) show attenuated weight loss and prolonged survival in NOD.SCID mice compared to the CB17.SCID control. Statistically significant difference in survival rates was obtained using Log-rank (Mantel-Cox) test. **(C)** Lungs were harvested from PR8 infected mice on day 5 post-infection and virus titer was measured by plaque assay. Pooled results from three groups of mice (n=5 per group) show no difference in virus titer between groups.

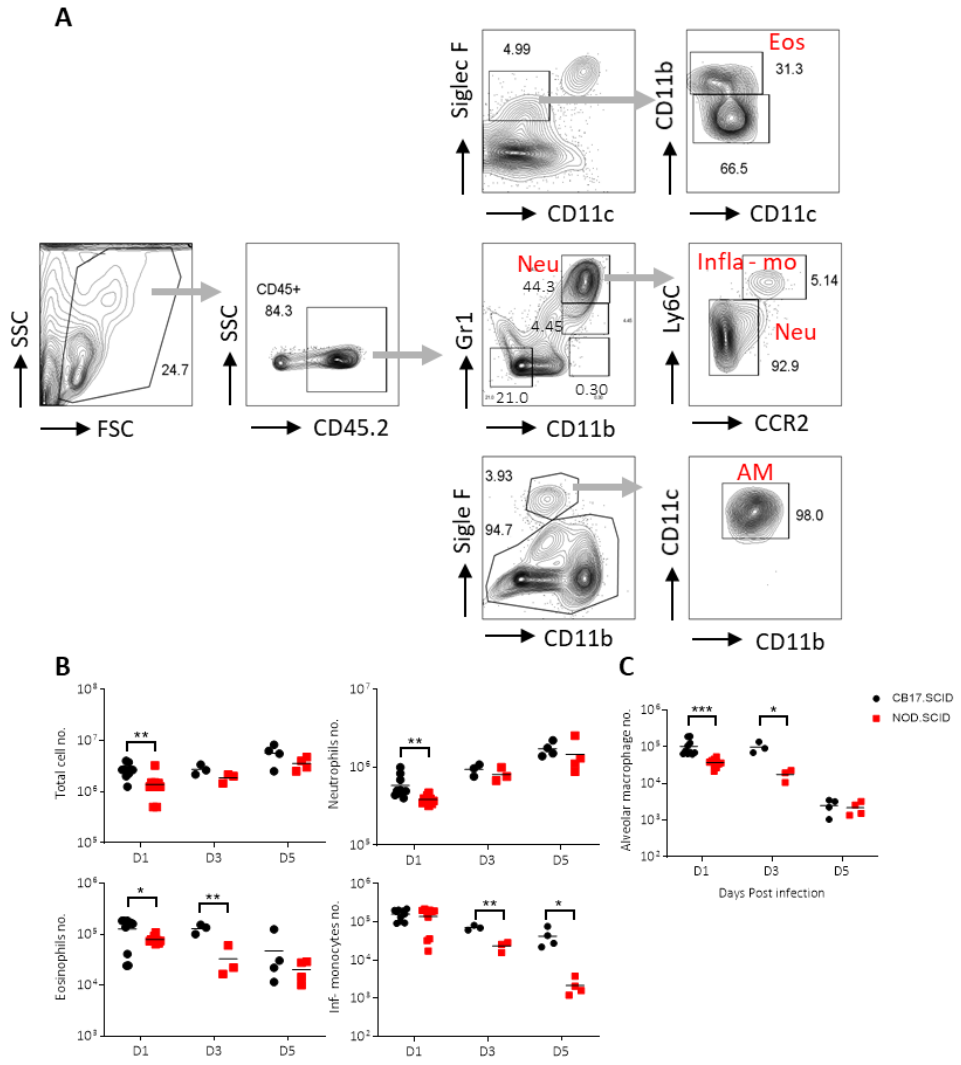

Figure 2. Comparative evaluation of innate immune cells in PR8-infected lungs of CB17.SCID and NOD.SCID mice by flow cytometry. **(A)** Gating strategy for flow cytometric analysis. (B) Cells were harvested from the lungs of CB17.SCID and NOD.SCID mice on day 1, 3 and 5 post-infection and the absolute number of each immune cells was calculated based on the results of flow cytometric analysis. Pooled results from two groups of mice (n=5 per group) show a statistically significant difference in the number of

immune cells between two groups. Statistical analysis was performed using unpaired t-test. *, $p < 0.05$; **, $p < 0.04$; ***, $p < 0.001$.

Higher *Cxcl14* gene expression in the lungs from influenza-infected NOD.SCID mice compared to CB17.SCID mice

To find a molecular signature associated with attenuated lung inflammation in influenza-infected NOD.SCID mice, mRNAs were extracted from the lungs of NOD.SCID and CB17.SCID mice one day after PR8 virus challenge and bulk RNA sequencing analysis was performed. Out of a total of 20,623 genes, 1,703 differentially expressed genes (DEGs) were filtered by p-value <0.05 and fold change >2 was obtained. 827 genes (49%) were significantly downregulated and 876 genes (51%) were significantly upregulated in NOD.SCID mice compared to CB17.SCID (Fig. 3A). To explore the major pathways associated with these DEGs, pathway analysis using Bioplanet 2019 (p-value ranking) in Enrichr (https://maayanlab.cloud/ Enrichr/) was performed, providing the top 10 up-regulated (Fig. 3B and Table 1) and down-regulated (Fig. 3C and Table 2) signaling pathways in NOD.SCID mice. In particular, cytokine-cytokine receptor interaction was the most dominantly downregulated pathway in NOD.SCID mice (Fig. 3 D & E). IFN type I (*ifna4, ifnb1*) and type III (*ifnl2, ifnl3*) are the early response cytokines secreted by pulmonary epithelial cells, alveolar macrophages and plasmacytoid dendritic cells in response to recognition of IAVs. Notably, the production of IFN-λ (*ifnl2, ifnl3*) is restricted in epithelial cells [6], suggesting that the pulmonary epithelial response to IAVs infection is reduced in NOD.SCID mice compared to CB17.SCID mice. IL-1 (*Il1a*, *Il1b*), IL-6 (*Il6*) and TNF-α (*Tnf*)

are early inflammatory cytokines. CCL2 (*Ccl2*) is the ligand for CCR2, which recruits $CCR2^{+}$ inflammatory monocytes [13]. CXCL1 (*Cxcl1*), CXCL2 (*Cxcl2*) and CXCL5 (*Cxcl5*) are the ligands of CXCR2, which induces neutrophil infiltration in influenza-infected lungs [31-33]. CXCL11 (*Cxcl11*), the ligand of CXCR3, is also involved in neutrophil recruitment [34]. CCL20 promotes the migration of immune cells such as monocytes, eosinophils and NK cells [35]. The downregulated expression of these chemokine genes in the lungs of NOD.SCID mice was further confirmed by quantitative real-time PCR (Fig. 4A).

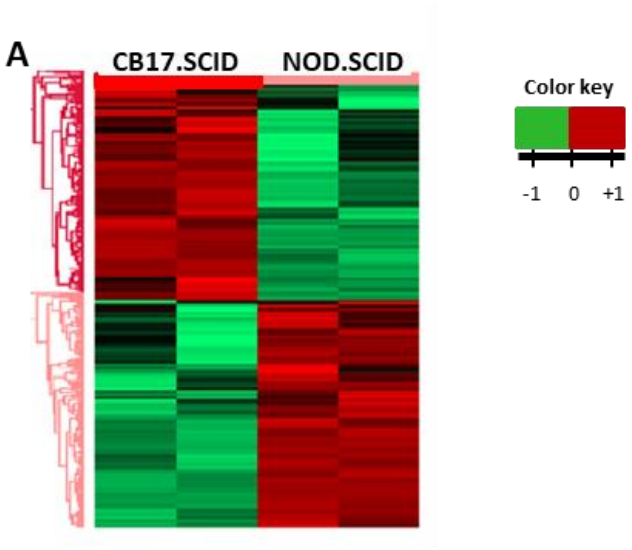
A
CB17.SCID
NOD.SCID
Color key
-1
0
+1

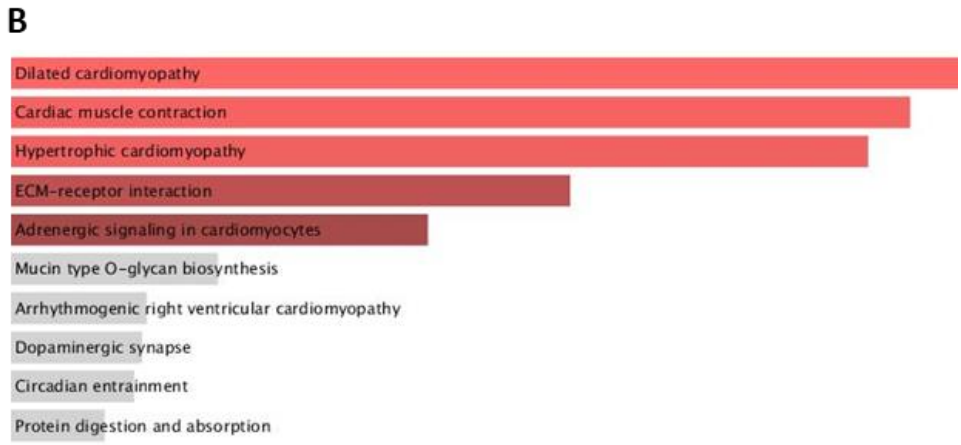
B
Dilated cardiomyopathy
Cardiac muscle contraction
Hypertrophic cardiomyopathy
ECM-receptor interaction
Adrenergic signaling in cardiomyocytes
Mucin type O-glycan biosynthesis
Arrhythmogenic right ventricular cardiomyopathy
Dopaminergic synapse
Circadian entrainment
Protein digestion and absorption

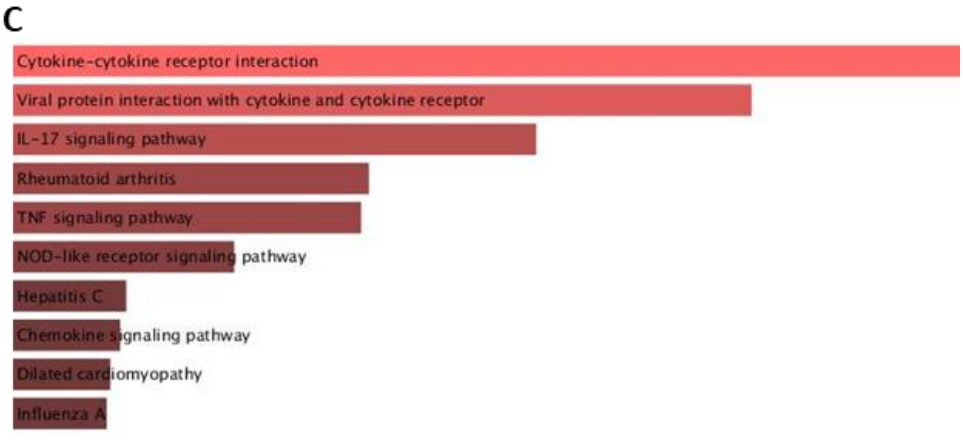
C
Cytokine-cytokine receptor interaction
Viral protein interaction with cytokine and cytokine receptor
IL-17 signaling pathway
Rheumatoid arthritis
TNF signaling pathway
NOD-like receptor signaling pathway
Hepatitis C
Chemokine signaling pathway
Dilated cardiomyopathy
Influenza A

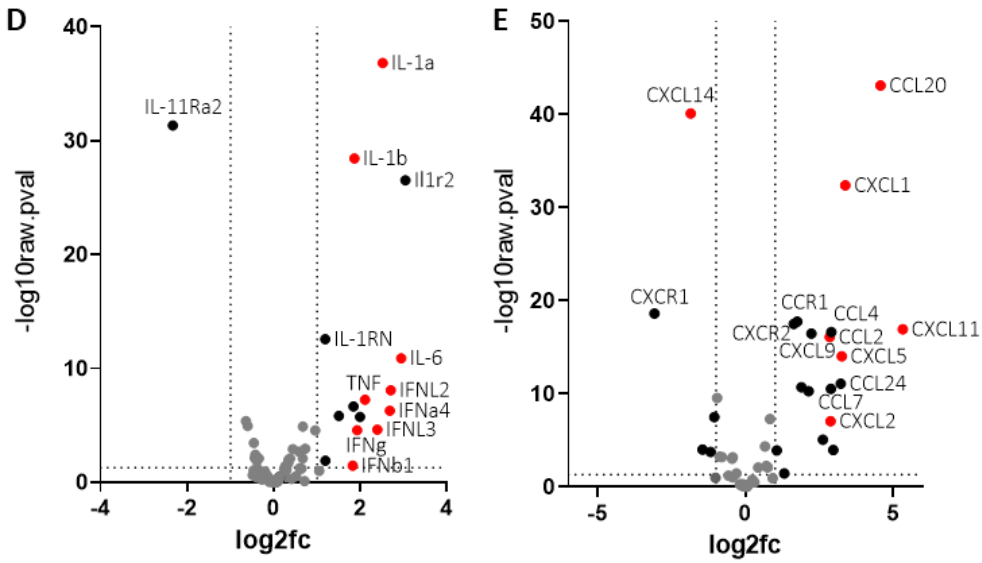

Figure 3. **Comparison of gene expression profile in the PR8-infected lungs of CB17.SCID and NOD.SCID mice.** Total mRNA was extracted from lungs on day 1 post-infection and bulk RNA sequencing analysis was performed. **(A)** Heat map of differentially expressed genes between CB17.SCID and NOD.SCID mice (n=2 per group) **(B-C)** Gene sets enriched in NOD.SCID (B) and CB17.SCID (C) mice were analyzed using Bioplanet 2019 (p-value ranking) in Enrichr, showing the top 10 dominant pathways in each mouse group. **(D-E)** Volcano plots showing differentially expressed cytokine (D) and chemokine (E) genes between two groups.

Table 2. Top 10 upregulated pathways in NOD.SCID versus CB17.SCID mouse lungs

Index	Name	P-value	Adjusted p-value	Odds Ratio	Combined score	Gene list
1	Dilated cardiomyopathy	0.0002788	0.04352	3.46	28.28	MYBPC3, RYR2, LAMA1, TNNC1, PLN, ACTC1, SGCA, TNNT2, MYL3, TNNI3, SGCG, MYH6, CACNG4
2	Cardiac muscle contraction	0.0003987	0.04352	3.53	27.61	MYL4, RYR2, ACTC1, TNNC1, TNNT2, MYL3, CASQ2, HRC, TNNI3, MYH6, CACNG4,TRDN
3	Hypertrophic cardiomyopathy	0.000563	0.04352	3.39	25.48	MYBPC3,RYR2,ACTC1,SGCA,LAMA1,TNNC1 ,TNNT2,MYL3,TNNI3,SGCG,MYH6,CACNG4
4	ECM-receptor interaction	0.005078	0.3034	2.82	14.9	GP9, GP1BB, LAMA1, CHAD, COL4AA6, TNR, GP1BA, HMMR, GP6, FREM2
5	Adrenergic signaling in cardiomyocytes	0.01474	0.7045	2.09	8.8	RYR2,TNNC1,CALML4,MYL4,PLN,ACTC1,PP P2R2C,TNNT2,MYL3,TNNI3,SCN5A,MYH6,C ACNG4
6	Mucin type O-glycan biosynthesis	0.07113	1	2.74	7.23	GALNT6, GALNT13, ST6GALNAC3, B3GNT3
7	Arrhythmogenic right ventricular cardiomyopathy	0.121	1	1.85	3.91	RYR2, SGCA, ACTN2, LAMA1, SGCG, CACNG4
8	Dopaminergic synapse	0.1256	1	1.6	3.33	MAPK10, KCNJ5, PPP2R2C, KIF5C, GNG8, CALML4, GRIN2B, SLC18A2, KCNJ3
9	Circadain entrainment	0.133	1	1.7	3.44	RYR2, KCNJ5, GNG8, CALML4, GRIN2B, RYR3, KCNJ3

10	Protein digestion and absorption	0.1656	1	1.6	2.87	COL17A1, COL26A1, CPB1, KCNE3, ELN, COL4A6, COL10A1

Table 3. Top 10 down-regulated pathways in NOD.SCID vs. CB17.SCID mouse lungs

Index	Name	P-value	Adjusted p-value	Odds Ratio	Combined score	Gene list
1	Cytokine-cytokine receptor interaction	4.34591E-10	1.217E-07	3.11	67.09	CXCL1,2,3,5,9,10,14 CCL2,3,11,20, IL-1α,1β,6
2	Viral protein interaction with cytokine and cytokine receptor	1.31409E-08	1.840E-06	4.85	87.97	CCR1,4, CXCL1,2,3,5,9,10,14, CCL2,3,4,7,11,20,22,24, IL-6, CXCR1,2
3	IL-17 signaling pathway	4.45607E-07	4.159E-05	4.38	63.99	CXCL1,2,3,5,10, CCL2,7,11,20, MMP3, FOSL1, MAPK10, IL-6,1β
4	Rheumatoid arthritis	6.88981E-06	4.381E-04	3.88	46.1	MMP3, CXCL1,2,3,5, CCL2,3,20, IL-1α,1β,6, IFNG,CTSK
5	TNF signaling pathway	7.82410E-06	4.381E-04	3.52	41.34	CXCL1,2,3,5,10, CCL2,20, MAPK1, SOCS3, IL-6,1β, IFNβ1, MMP3
6	NOD-like receptor signaling pathway	6.24451E-05	2.914E-03	2.59	25.12	CXCL1,2,3, CCL2, GBP2,3,5,7, IFNβ1, STAT2, IL-6, NLRP12 ,IL-1β, MYD88
7	Hepatitis C	3.65516E-04	1.409E-02	2.49	19.74	IFNA4, CDKN1A, RSAD2,IFNβ1, STAT2, IFIT1, SOCS3, CLDN4,6, OAS2,3
8	Chemokine signaling pathway	4.03433E-04	1.409E-02	2.31	18.05	CXCL10, IFNA4, IFNβ1, STAT2, IFIT1, SOCS3, CLDN4,6, IAS2,3
9	Dilated cardiomyopathy	4.74639E-04	1.409E-02	2.98	22.84	MYBPC3, RYR2, LAMA1, TNNC1, ADCY4, PLN, ACTC1, SGCA, TNNT2

10	Influenza A	5.03161E-04	1.409E-02	2.37	17.99	MYBPC3, RYR2, LAMA1, TNNC1, TNF, IL-6, ACTC1, SGCA, TNNT2, MYL3

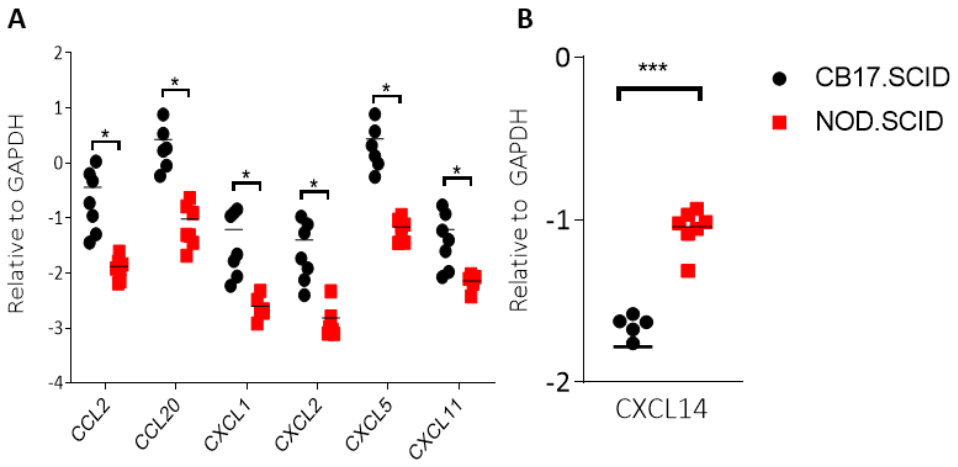

Fig. 4 Comparative analysis of the expression of selected chemokine genes between the lungs of CB17.SCID and NOD.SCID mice infected with PR8. Total mRNAs were extracted from infected lungs of CB17.SCID and NOD.SCID mice, and the transcript levels of each gene were measured by quantitative reverse transcription real-time PCR, and the relative gene expression level was calculated using *Gapdh* as a control gene. (A) Summarized results from two groups of mice (n=7 per group) showed statistically significantly upregulated chemokine genes in CB17.SCID lungs compared with those of NOD.SCID mice. (B) Summarized graph obtained from the same set as A shows higher expression of *Cxcl14* chemokine genes in NOD.SCID lung than CB17.SCID control. *, $p < 0.05$; ***, $p < 0.001$

Protection of mice against lethal influenza infection by inoculation with AAV9-EGFP vector

In contrast to many inflammatory cytokines, RNA sequencing analysis revealed an upregulation of some cytokine and chemokine genes, in particular the *Cxcl14* gene, in NOD.SCID mice compared to the CB17.SCID control (Fig. 3E). Quantitative real-time PCR analysis confirmed that *Cxcl14* gene expression was significantly higher in NOD.SCID than in CB17.SCID (Fig. 4B). *CXCL14* is a 9.4 kDa chemokine produced by a variety of immune and non-immune cells, including airway epithelial cells, and exerts diverse functions such as modulation of leukocyte migration and differentiation and antimicrobial activity [36, 37]. Notably, *CXCL14* has been reported to inhibit M1 macrophage polarization and proinflammatory cytokine production in a sepsis-associated kidney injury model [38]. This raised the possibility that overexpression of *CXCL14* might also contribute to the suppression of lung inflammation following influenza infection in NOD.SCID mice. To investigate this, the *Cxcl14* gene was delivered to the lungs of mice using the AA9-EGFP vector. The non-pathogenicity and very low immunogenicity of AAV is known to allow long-term expression of therapeutic genes in both animals and humans [20, 21]. In particular, the AAV9-EGFP vector has recently been used to transduce the human ACE2 gene into mouse airway epithelial cells for the development of a SARS-CoV-2 mouse infection model [39]. Based on this, AAV9-EGFP-mCXCL14 vector was delivered into the

lungs of BALB/c mice by oropharyngeal inoculation, followed by intranasal infection with a lethal dose of PR8 IAVs. Mice receiving or not receiving the AAV9-EGFP control vector were also challenged with PR8 virus as a negative control. Increased *Cxcl14* gene expression in AAV9-EGFP-mCXC14 inoculated lungs was confirmed by qPCR prior to IAV infection (Fig. 5A). After IAV infection, survival time and rate were compared between mice in these three groups. First, mice were infected 2 weeks after AAV9 inoculation according to a previously reported protocol [39]. However, no difference in survival time and rate was observed between these three groups (Fig. 5B). Next, the time interval between vector inoculation and influenza infection was extended to 4 weeks because it had been reported that the expression of the AAV-transduced gene in the mouse increases progressively for more than 12 weeks after intravenous injection of the vectors [40]. Unexpectedly, both mice receiving AAV9-EGFP control or AAV9-EGFP-mCXCL14 vectors showed statistically significant survival rates and times compared to naive control mice infected with IAVs; 50% (5/10) and 40% (4/10) of mice receiving AAV9-EGFP or AAV9-EGFP-mCXCL14 vectors, respectively, were protected from lethal influenza infection, whereas naive mice showed 100% mortality (Fig. 5C). In addition, morbidity was also attenuated in these two groups of vector-treated mice in terms of weight loss compared to the naive control (Fig. 5D).

Next, inflammatory cells in the lungs of AAV9-EGFP vector-treated

mice and naive control mice were analyzed by flow cytometry just before PR8 infection (day 0) and on days 2 and 4 after infection (Fig. 6A). At day 0, there were higher numbers of monocytes ($Ly6C^-$ or $Ly6C^+$), NK cells, CD8 T cells and B cells in AAV9 vector administrated group than naïve control, while at day 4 post-infection there was a significant difference in the number of trans-macrophages and neutrophils between the two groups (Fig. 6B). Infiltration of trans-macrophages and neutrophils into the infected lungs was attenuated in AAV9 vector-treated mice compared to naïve mice. The number of NK cells was still higher in the AAV9 vector group on day 2 post infection. The number of other immune cells, including alveolar macrophages, eosinophils and CD4 T cells, did not differ between the two groups. In addition, gene expression levels of cytokines, including IFN-β, and chemokines were found to be comparable in the lungs of both groups of mice (Fig. 7). Finally, to assess whether AAV9 vector inoculation affected PR8 virus replication or clearance, lung viral titers were measured by qPCR and no difference was found between the two groups (Fig. 8). Taken together, these results suggest that pulmonary AAV9-EGFP vector inoculation may protect mice against lethal influenza infection by inhibiting neutrophil and/or trans-macrophage migration into the infected lung.

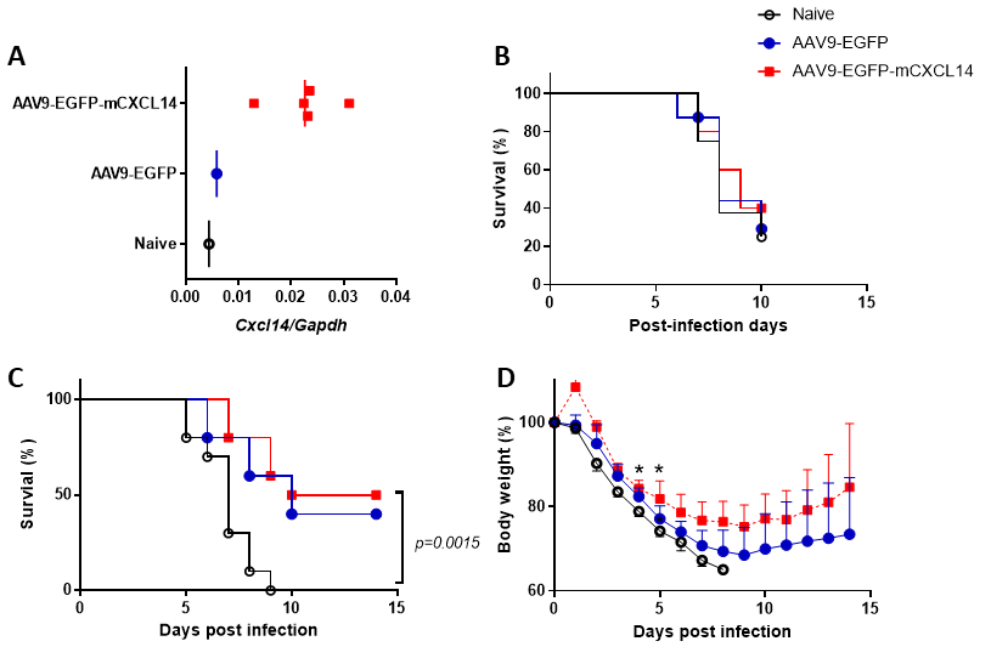

Fig 5. Mice protected from lethal influenza infection by airway inoculation of AAV9 vector. (A) AAV9-EGFP or AAV9-EGFP-mCXCL14 vectors were administered to BALB/c mice and lung *Cxcl14* gene expression was quantified by qPCR. Naive mice were used as negative controls. **(B)** Mice were infected with PR8 IAV 2 weeks after AAV9 vector inoculation. Naive mice were infected with PR8 virus as a control. Summarized survival graph of three groups (n=5 per group) showing no difference between groups. **(C-D)** Mice were infected with PR8 virus 4 weeks after AAV9 vector administration. Cumulative follow-up results from two independent experiments (n=10 per group) showed reduced mortality (B) and attenuated weight loss (C) in mice receiving AAV9-EGFP or AAV9-EGFP-mCXCL14 vectors compared to infected naive control. Statistical analysis was performed

using log-rank (Mantel-Cox) test and multiple t-test for comparison of survival and weight change, respectively. *, $p < 0.05$

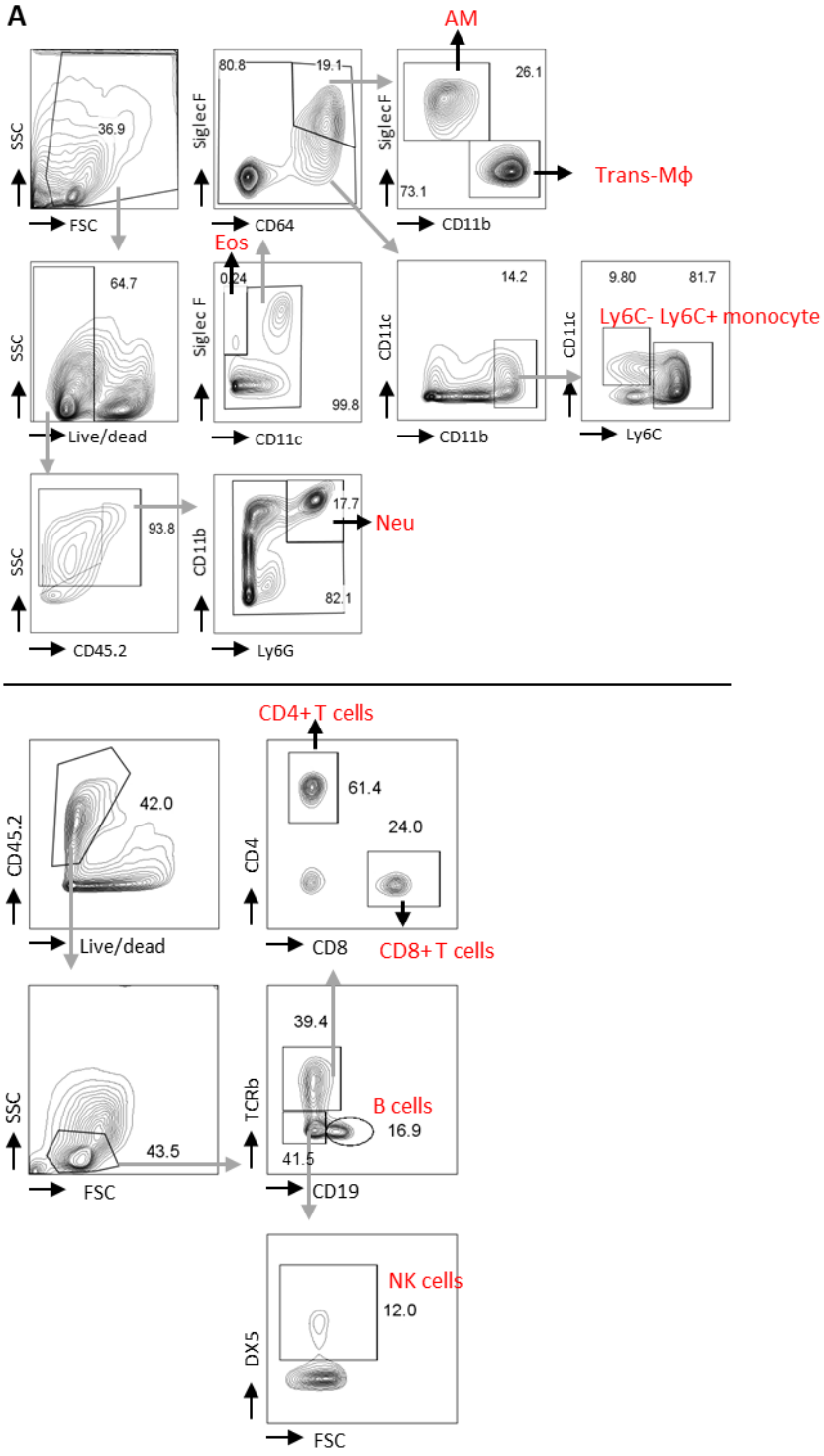
A
AM
SSC
36.9
FSC
80.8
19.1
SiglecF
CD64
26.1
73.1
SiglecF
CD11b
Trans-Mϕ
Eos
64.7
SSC
Live/dead
0.24
99.8
Siglec F
CD11c
14.2
CD11c
CD11b
9.80
81.7
CD11c
Ly6C
Ly6C- Ly6C+ monocyte
93.8
SSC
CD45.2
17.7
82.1
CD11b
Ly6G
Neu
CD4+T cells
42.0
CD45.2
Live/dead
61.4
24.0
CD4
CD8
CD8+T cells
39.4
B cells
16.9
41.5
TCRb
CD19
43.5
SSC
FSC
NK cells
12.0
DX5
FSC

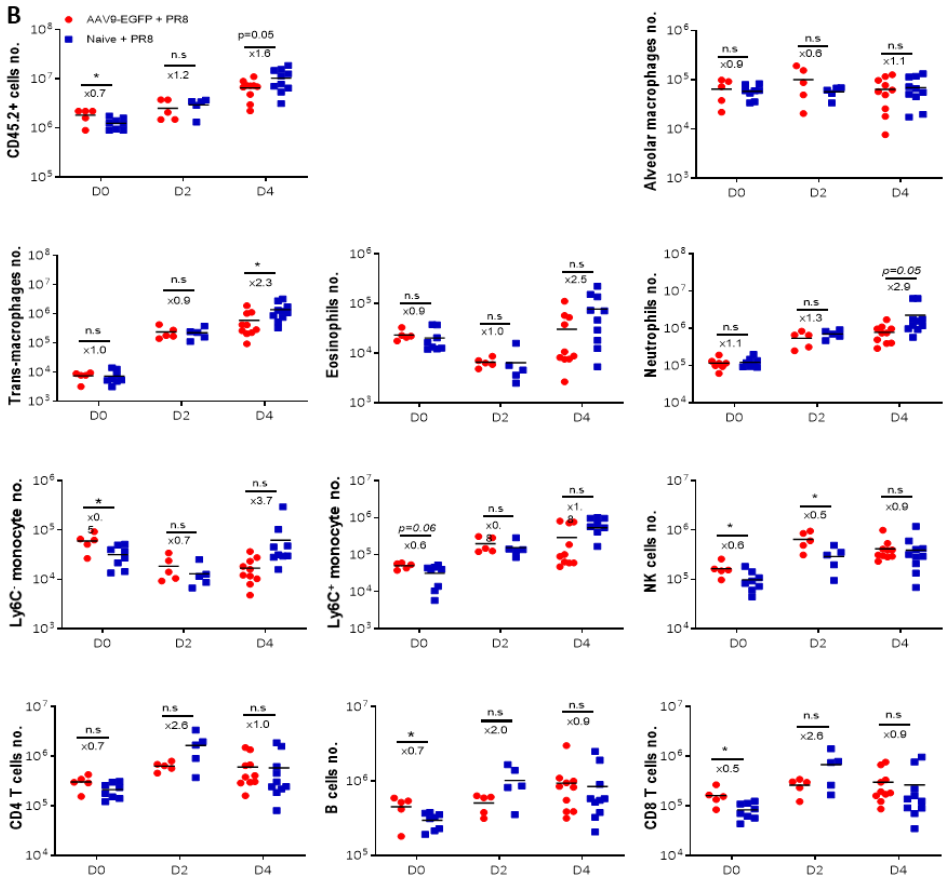

Figure 6. Reduced neutrophil and trans-macrophage infiltration in PR8-infected lungs of AAV9-EGFP vector-treated mice. (A) Strategy for gating immune cells in PR8-infected lungs by flow cytometry. **(B)** Cells were isolated from mouse lungs before PR8 infection (D0) or on days 2 (D2) and 4 (D4) post-infection 4 weeks after AAV9-EGFP vector administration and the absolute numbers of each immune cell were calculated based on the results of flow cytometry analysis. Naive mice infected without pre-administered AAV9 vector were used as controls. Cumulative results of two independent experiments (n= 5 ~10 per group) show lower numbers of

neutrophils and trans-macrophages at day 4 post-infection in the lungs of AAV9 vector-treated mice than in the naive control. *, $p < 0.05$

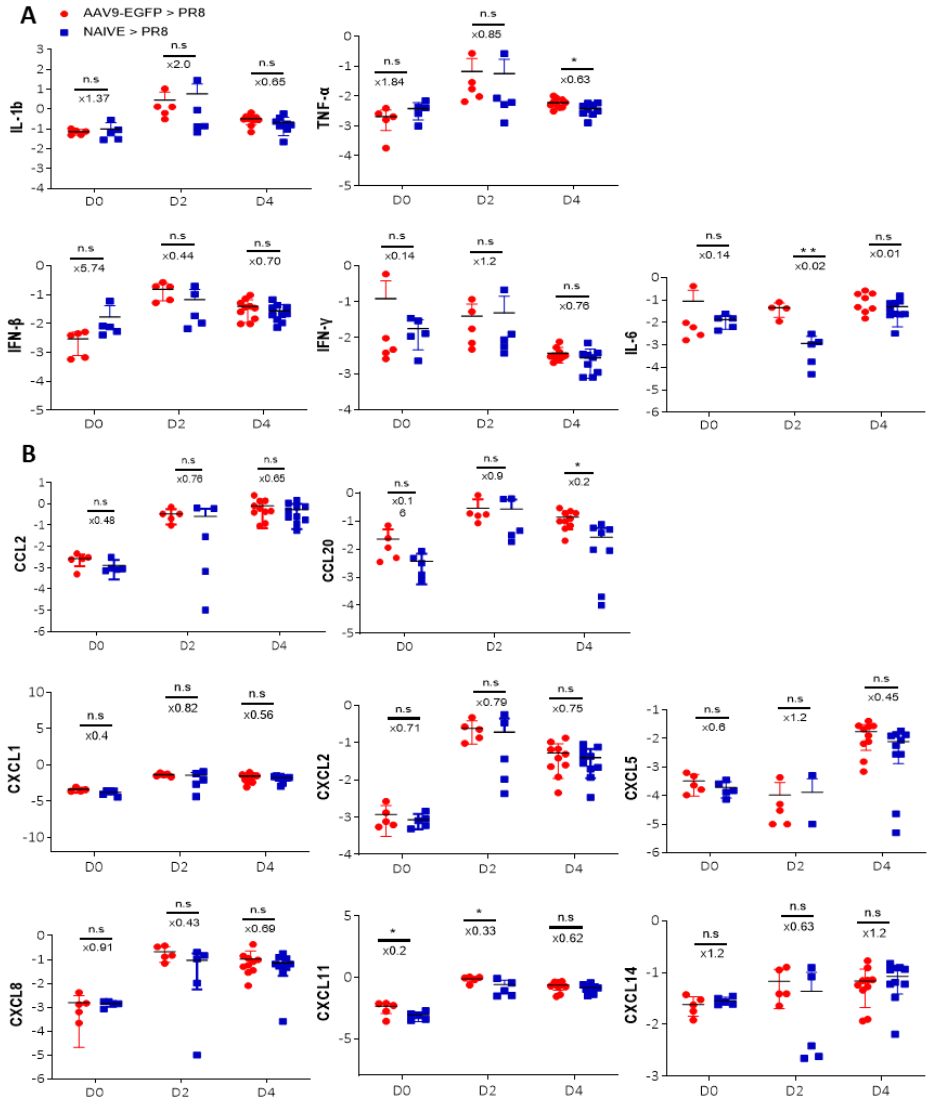

Figure 7. Chemokine gene expression in AAV9 vector administrated and naïve mouse lungs before and after PR8 infection. Total mRNA was extracted from mouse lungs before PR8 infection (D0) or on days 2 (D2) and 4 (D4) post-infection 4 weeks after AAV9-EGFP vector administration, and relative cytokine (**A**) and chemokine (**B**) gene expression levels were quantified by qPCR. The *Gapdh* gene was used to normalize the qPCR data.

Naive mice infected without pre-administered AAV9 vector were used as controls. Cumulative results of two independent experiments (n= 5 ~10 per group) show no significant difference between two groups.

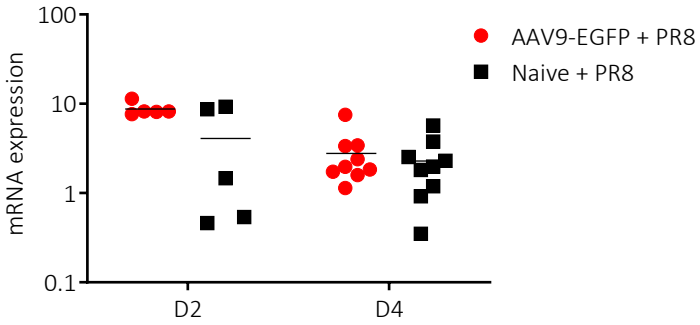

Figure 8. Comparison of IAV gene expression levels in mice receiving or not receiving AAV9 vector prior to PR8 virus infection. Total mRNAs were extracted from the lungs of mice infected with PR8 virus in the presence or absence of pre-administered AAV9 vector. Levels of PR8 virus N gene transcripts were measured by quantitative PCR. *Gapdh* was used as a control gene to calculate relative expression. Cumulative results from two independent experiments (n= 5 ~10 per group) show no difference in PR8 gene expression levels in two groups of mice.

.

DISCUSSION

In this study, I aimed to find the modalities to control influenza-associated lung injury and thereby protect the host from lethal influenza infection. Firstly, the innate immune response was compared between CB17.SCID and NOD.SCID mice and it was found that attenuated infiltration of neutrophils and inflammatory monocytes was associated with reduced morbidity and mortality in NOD.SCID mice compared to CB17.SCID mice. In addition, there was an increase in *Cxcl14* chemokine gene expression in infected NOD.SCID lungs. Based on these findings, *Cxcl14* gene was delivered to the lungs of mice using AAV9-EGFP vector to assess whether *Cxcl14* overexpression could alleviate inflammatory cell infiltration in IAV-infected lungs. Unfortunately, mice that received an AAV9 vector containing the *Cxcl14* gene prior to IAV infection showed similar morbidity in terms of weight loss and mortality to mice that received a control AAV9 vector. However, approximately half of the hosts in both groups survived, whereas all naive mice that did not receive the AAV9 vector died early after IAV challenge. Further analysis also showed that AAV9 vector inoculation into the respiratory tract led to a decrease in neutrophil and trans-macrophage infiltration in the infected lungs.

When BALB/c, CB17.SCID and NOD.SCID mice were infected with PR8 IAV, only BALB/c mice recovered after initial weight loss, while both

CB17.SCID and NOD.SCID, which lack adaptive immune cells, failed to survive due to failure of virus control, as expected. Furthermore, there was no difference in weight loss between BALB/c and CB17.SCID mice for the first 5 days, during which time adaptive immunity may not be fully activated to participate in virus control [6]. However, NOD.SCID mice showed a slower decrease in body weight and longer survival time than CB17.SCID mice, while virus titre was similar in all three groups. Flow cytometric analysis revealed that exaggerated infiltration of neutrophils and inflammatory monocytes was associated with severe morbidity and shortened survival in CB17.SCID mice. These findings support previous reports that attenuation of neutrophil and monocyte infiltration in influenza-infected lungs has beneficial effects on host morbidity and mortality [11, 13, 14].

One of the notable findings in the initial experiments of this study was an inverse correlation between the expression level of the *Cxcl14* gene and the degree of inflammatory cell influx in infected lungs. *CXCL14* has previously been suggested to have an anti-inflammatory effect [38, 41]. However, TNF-α could downregulate *Cxcl14* expression and *CXCL14* deficiency was reported not to affect the severity of IAV infection [42, 43]. In the current study, TNF-α levels were much higher in severely inflamed CB17.SCID lungs compared to NOD.SCID lungs, and *Cxcl14* gene delivery using AAV9 vectors into the mouse airway failed to show beneficial effects of *CXCL14* chemokine on the survival of IAV-infected hosts. These results

suggest that the high level of *Cxcl14* expression in the infected lung of NOD.SCID may result from low levels of TNF-α rather than reflect the anti-inflammatory effect of this chemokine.

Here, administration of AAV9 vectors containing only EGFP, which are usually used as control vectors in gene transfer experiments with AAV9 vectors, showed a prophylactic effect against lethal influenza infection. More interestingly, this effect was observed when the AAV9 vector was inoculated only 4 weeks but not 2 weeks before PR8 IAV infection. According to a previous report, intranasal instillation of replication-deficient adenovirus (E1 & E3 gene-deleted Ad5 empty, AdE) particles without transgene also protected BALB/c mice against lethal PR8 infection [44]. However, AdE particles were administered 2 days prior to PR8 challenge and their effect was thought to be due to rapid induction of inflammatory cytokines/chemokines and antiviral response, although the actual action mechanisms were not well understood. In contrast to adenovirus particles, AAV vectors are known not to induce acute inflammation [21]. Moreover, the main feature observed in AAV9-treated mice of the current study was an attenuated infiltration of neutrophils and trans-macrophages in PR8-infected lungs, suggesting that the prophylactic mechanisms of AAV9 and AdE may be different.

Although AAV vectors are usually poorly immunogenic, their immunogenicity is dose-dependent and adaptive immune responses against

the transgene product and viral cap protein could limit their long-term efficacy [21, 45]. Innate immunity could also be triggered by the double-stranded DNA (dsDNA) vector genome [45]. In addition, a previous interesting study showed that dsRNA transcribed from viral dsDNA could promote IFN-β production in host cells [25]. According to this report, IFN-β could suppress AAV transgene expression in vivo and in vitro, and IFN-β production in host cells was dependent on the MDA5 dsRNA sensor, suggesting that dsRNA could trigger IFN-β production. This possibility was further confirmed by demonstrating the presence of transgene-derived minus strand transcripts, which are essential for dsRNA formation. Notably, the level of IFN-β induction in humanized mice was higher 8 weeks than 4 weeks after injection of the AAV vector carrying the human Factor IX gene. Considering that transgene expression levels increase progressively after gene delivery using AAV vectors, especially for more than 12 weeks in mice [40], it was suggested that IFN-β induction levels correlate with transgene expression levels. Taken together, this could explain why the prophylactic effect of the AAV9 vector was found 4 weeks rather than 2 weeks after vector administration in the current study.

This study has certain limitations in terms of understanding the prophylactic mechanism of the AAV9 vector. The current study did not thoroughly document the specific mechanisms involved. While the increased infiltration of monocytes, NK cells and CD8 T cells in the lungs of AAV9-

inoculated mice may contribute to early viral control, no significant difference in viral gene expression levels was observed between the AAV9 and control groups. Alternative explanations could include IFN-β production triggered by dsRNA generated from the transgene, which may induce antiviral genes in the alveolar epithelium, the primary host cell of the AAV9 vector. Another possibility is that long-term exposure to low levels of IFN-β may lead to desensitization of innate immune cells. However, no significant increase in IFN-β gene expression was observed in AAV9 vector-treated mice compared to naive control mice. To re-evaluate this finding, it is crucial to assess the expression of the IFN-β gene specifically in isolated lung epithelial cells and to investigate the potential elimination of the protective effect of the AAV9 vector by blocking IFN-β activity. In addition, studies depleting neutrophils or monocytes could clarify whether the presence of these cells is necessary for the protective effect of the AAV vector. Nevertheless, this study represents the first report demonstrating the protective effect of the AAV vector in a severe influenza model.

REFERENCES

1. Dawson, W.K., M. Lazniewski, and D. Plewczynski, *RNA structure interactions and ribonucleoprotein processes of the influenza A virus.* Brief Funct Genomics, 2018. **17**(6): p. 402-414.
2. Shao, W., et al., *Evolution of Influenza A Virus by Mutation and Re-Assortment.* Int J Mol Sci, 2017. **18**(8).
3. Smith, G.J., et al., *Dating the emergence of pandemic influenza viruses.* Proc Natl Acad Sci U S A, 2009. **106**(28): p. 11709-12.
4. Gu, Y., et al., *The Mechanism behind Influenza Virus Cytokine Storm.* Viruses, 2021. **13**(7).
5. Perrone, L.A., et al., *H5N1 and 1918 pandemic influenza virus infection results in early and excessive infiltration of macrophages and neutrophils in the lungs of mice.* PLoS Pathog, 2008. **4**(8): p. e1000115.
6. Irene Latino, S.F.G., *Spatio-temporal profile of innate inflammatory cells and mediators during influenza virus infection.* current opinion in physiology, 2021. **19**.
7. George, S.T., et al., *Neutrophils and Influenza: A Thin Line between Helpful and Harmful.* Vaccines (Basel), 2021. **9**(6).
8. Peiro, T., et al., *Neutrophils drive alveolar macrophage IL-1beta release during respiratory viral infection.* Thorax, 2018. **73**(6): p.

546-556.

9. Tate, M.D., et al., *Neutrophils sustain effective CD8(+) T-cell responses in the respiratory tract following influenza infection.* Immunol Cell Biol, 2012. **90**(2): p. 197-205.

10. Lim, K., et al., *Neutrophil trails guide influenza-specific CD8(+) T cells in the airways.* Science, 2015. **349**(6252): p. aaa4352.

11. Brandes, M., et al., *A systems analysis identifies a feedforward inflammatory circuit leading to lethal influenza infection.* Cell, 2013. **154**(1): p. 197-212.

12. Palomino-Segura, M., et al., *Protection against influenza infection requires early recognition by inflammatory dendritic cells through C-type lectin receptor SIGN-R1*. Nat Microbiol, 2019. **4**(11): p. 1930-1940.

13. Lin, S.J., et al., *The pathological effects of CCR2+ inflammatory monocytes are amplified by an IFNAR1-triggered chemokine feedback loop in highly pathogenic influenza infection.* J Biomed Sci, 2014. **21**(1): p. 99.

14. Coates, B.M., et al., *Inflammatory Monocytes Drive Influenza A Virus-Mediated Lung Injury in Juvenile Mice.* J Immunol, 2018. **200**(7): p. 2391-2404.

15. Li, F., et al., *Monocyte-derived alveolar macrophages autonomously determine severe outcome of respiratory viral infection.* Sci Immunol,

2022. **7**(73): p. eabj5761.

16. Duan, M., M.L. Hibbs, and W. Chen, *The contributions of lung macrophage and monocyte heterogeneity to influenza pathogenesis.* Immunol Cell Biol, 2017. **95**(3): p. 225-235.

17. Narasaraju, T., et al., *Excessive neutrophils and neutrophil extracellular traps contribute to acute lung injury of influenza pneumonitis.* Am J Pathol, 2011. **179**(1): p. 199-210.

18. Somerville, L., A. Cardani, and T.J. Braciale, *Alveolar Macrophages in Influenza A Infection Guarding the Castle with Sleeping Dragons.* Infect Dis Ther (San Antonio), 2020. **1**(1).

19. Lin, K.L., et al., *CCR2-antagonist prophylaxis reduces pulmonary immune pathology and markedly improves survival during influenza infection.* J Immunol, 2011. **186**(1): p. 508-15.

20. Kessler, P.D., et al., *Gene delivery to skeletal muscle results in sustained expression and systemic delivery of a therapeutic protein.* Proc Natl Acad Sci U S A, 1996. **93**(24): p. 14082-7.

21. Zaiss, A.K. and D.A. Muruve, *Immune responses to adeno-associated virus vectors.* Curr Gene Ther, 2005. **5**(3): p. 323-31.

22. Li, C. and R.J. Samulski, *Engineering adeno-associated virus vectors for gene therapy.* Nat Rev Genet, 2020. **21**(4): p. 255-272.

23. McCarty, D.M., *Self-complementary AAV vectors; advances and applications.* Mol Ther, 2008. **16**(10): p. 1648-56.

24. Au, H.K.E., M. Isalan, and M. Mielcarek, *Gene Therapy Advances: A Meta-Analysis of AAV Usage in Clinical Settings.* Front Med (Lausanne), 2021. **8**: p. 809118.

25. Shao, W., et al., *Double-stranded RNA innate immune response activation from long-term adeno-associated virus vector transduction.* JCI Insight, 2018. **3**(12).

26. Jhappan, C., et al., *DNA-PKcs: a T-cell tumour suppressor encoded at the mouse scid locus.* Nat Genet, 1997. **17**(4): p. 483-6.

27. Serreze, D.V., J.W. Gaedeke, and E.H. Leiter, *Hematopoietic stem-cell defects underlying abnormal macrophage development and maturation in NOD/Lt mice: defective regulation of cytokine receptors and protein kinase C.* Proc Natl Acad Sci U S A, 1993. **90**(20): p. 9625-9.

28. Ogasawara, K., et al., *Impairment of NK cell function by NKG2D modulation in NOD mice.* Immunity, 2003. **18**(1): p. 41-51.

29. Channappanavar, R., et al., *Dysregulated Type I Interferon and Inflammatory Monocyte-Macrophage Responses Cause Lethal Pneumonia in SARS-CoV-Infected Mice.* Cell Host Microbe, 2016. **19**(2): p. 181-93.

30. Cardani, A., et al., *Alveolar Macrophages Prevent Lethal Influenza Pneumonia By Inhibiting Infection Of Type-1 Alveolar Epithelial Cells.* PLoS Pathog, 2017. **13**(1): p. e1006140.

31. Ferrero, M.R., et al., *CCR5 Antagonist Maraviroc Inhibits Acute Exacerbation of Lung Inflammation Triggered by Influenza Virus in Cigarette Smoke-Exposed Mice.* Pharmaceuticals (Basel), 2021. **14**(7).

32. Tavares, L.P., et al., *CXCR1/2 Antagonism Is Protective during Influenza and Post-Influenza Pneumococcal Infection.* Front Immunol, 2017. **8**: p. 1799.

33. Duemmler, A., et al., *CXCL5 into the upper airways of children with influenza A virus infection.* Rev Med Inst Mex Seguro Soc, 2010. **48**(4): p. 393-8.

34. Rudd, J.M., et al., *Neutrophils Induce a Novel Chemokine Receptors Repertoire During Influenza Pneumonia.* Front Cell Infect Microbiol, 2019. **9**: p. 108.

35. Luo, C., et al., *Dynamic analysis of expression of chemokine and cytokine gene responses to H5N1 and H9N2 avian influenza viruses in DF-1 cells.* Microbiol Immunol, 2018. **62**(5): p. 327-340.

36. Lu, J., et al., *CXCL14 as an emerging immune and inflammatory modulator.* J Inflamm (Lond), 2016. **13**: p. 1.

37. Shaykhiev, R., et al., *Smoking-induced CXCL14 expression in the human airway epithelium links chronic obstructive pulmonary disease to lung cancer.* Am J Respir Cell Mol Biol, 2013. **49**(3): p. 418-25.

38. Lv, J., et al., *CXCL14 Overexpression Attenuates Sepsis-Associated Acute Kidney Injury by Inhibiting Proinflammatory Cytokine*

Production. Mediators Inflamm, 2020. **2020**: p. 2431705.

39. Israelow, B., et al., *Mouse model of SARS-CoV-2 reveals inflammatory role of type I interferon signaling.* J Exp Med, 2020. **217**(12).

40. Palomeque, J., et al., *Efficiency of eight different AAV serotypes in transducing rat myocardium in vivo.* Gene Ther, 2007. **14**(13): p. 989-97.

41. Rajasekaran, G., et al., *Antimicrobial and anti-inflammatory activities of chemokine CXCL14-derived antimicrobial peptide and its analogs.* Biochim Biophys Acta Biomembr, 2019. **1861**(1): p. 256-267.

42. Maerki, C., et al., *Potent and broad-spectrum antimicrobial activity of CXCL14 suggests an immediate role in skin infections.* J Immunol, 2009. **182**(1): p. 507-14.

43. Sidahmed, A.M., et al., *CXCL14 deficiency does not impact the outcome of influenza or Escherichia coli infections in mice.* J Infect Dev Ctries, 2014. **8**(10): p. 1301-6.

44. Zhang, J., et al., *Adenovirus-vectored drug-vaccine duo as a rapid-response tool for conferring seamless protection against influenza.* PLoS One, 2011. **6**(7): p. e22605.

45. Verdera, H.C., K. Kuranda, and F. Mingozzi, *AAV Vector Immunogenicity in Humans: A Long Journey to Successful Gene Transfer.* Mol Ther, 2020. **28**(3): p. 723-746.

국문 초록

인플루엔자 A 바이러스(IAV)는 오랫동안 인간을 위협했고 때로는 높은 발병률과 사망률을 일으켰다. 첫 번째 면역반응은 감염된 상피세포, 폐포대식세포 그리고 수지상세포에 의해 촉발되고, 이어 바이러스 복제를 억제하는 선천성 면역세포가 침투해 적응 면역이 나타나기 전 바이러스의 확산을 억제한다. 하지만 과도한 선천성 면역반응은 심각한 폐 손상을 일으켜 숙주를 사망까지 일으킬 수 있다. 특히 중증 인플루엔자에 걸린 숙주의 폐에서 관찰되는 주요 병리는 호중구와 염증성 단핵구의 대량 유입이다. 본 연구에서는 중증 인플루엔자 감염 후 발생하는 과도한 면역반응에 의한 폐 손상을 제어할 수 있는 방안을 찾아보고자 하였다.

후천면역반응이 결핍된 CB17.SCID와 NOD.SCID 마우스에 A형인플루엔자바이러스(PR8)를 감염시켰을 때, 단핵구·대식세포 발달과 자연살해세포 기능에 결함이 있는 NOD.SCID 마우스는 CB17.SCID 마우스에 비해 체중감소가 현저히 덜하였고, 사망률도 낮았다. 감염된 폐조직에서 세포를 분리하여 시행한 유세포분석 분석에 따르면, 호중구와 염증성 단핵구 침윤의 감소가 NOD.SCID 마우스에서 생존율 향상과 연관이 있었다. 또한 많은 염증성 사이토카인 및 케모카인 유전자 발현 수준도 CB17.SCID 보다 NOD.SCID 마우스의 감염된 폐에서 통계학적으로 유의하게 낮았다. 그러나 *Cxcl14* 케모카인

유전자 발현은 NOD.SCID 폐에서 더 높았다. 이를 바탕으로 아데노관련바이러스-9(AAV9) 벡터를 유전자 전달계로 활용해 마우스 폐에서 *Cxcl14* 케모카인의 발현 증가가 치명적인 인플루엔자 감염으로부터 숙주를 보호할 수 있는지 조사하였다. 흥미롭게도 AAV9-EGFP 대조군 벡터와 AAV9-EGFP-mCXCL14 실험군 벡터를 투여한 두 군 모두에서 AAV 벡터를 투여하지 않은 대조군 마우스에 비해 마우스 사망률이 크게 감소하였다. 그리고, 유세포분석으로 호중구와 전이대식세포(trans-macrophage)가 AAV9 투여군의 감염된 폐에서 감소되어 있음을 확인하였다. 그러나, 세 군의 마우스 간에 바이러스 유전자 전사 수준에는 차이가 보이지 않았다. 이전 보고서에 따르면, AAV 벡터의 독특한 게놈 구조가 AAV 도입 세포의 세포질에서 바이러스 게놈으로부터 이중 사슬 RNA를 생성하고 MDA5 의존적으로 인터페론-베타를 생성할 수 있다는 것을 고려할 때, 본 연구결과는 AAV 벡터 투여가 선천면역반응에 영향을 주어서 인플루엔자 감염 후 과도한 폐손상을 억제할 수 있음을 시사한다.